Available online at www.sciencedirect.com

ScienceDirect

Procedia CIRP 121 (2024) 97–102

www.elsevier.com/locate/procedia

11th CIRP Global Web Conference (CIRPe 2023)

Tool wear for finishing milling of green thermoplastic-ceramic composites fabricated with pellet AM

Laurent Spitaels[a,*], Naiara Aldeiturriaga Olabarri[a,b], Julien Bossu[a], Gregory Martic[c], Enrique Juste[c], Pedro-José Arrazola[b], Édouard Rivière-Lorphèvre[a], François Ducobu[a]

[a]*Research Institute for Science and Material Engineering - University of Mons, Place du Parc 20, Mons 7000, Belgium*
[b]*Mondragon Unibertsitatea, Faculty of Engineering, Loramendi 4, Arrasate-Mondragón, 20500, Spain*
[c]*Belgium Ceramic Research Centre, Avenue Gouverneur Cornez 4, Mons 7000, Belgium*

* Corresponding author. *E-mail address:* laurent.spitaels@umons.ac.be

Abstract

The wear of milling tools used for finishing green ceramics shaped by pellet additive manufacturing can be challenging. This article aims to evaluate the tool life of a tool, initially dedicated to thermoplastics, when used for milling green zirconia and seeks to confirm the influence of the build direction on the cutting forces. The tool can withstand 30 minutes of milling without reaching the tool life criteria of ISO 8688. The generated surfaces exhibited a shiny finish, no material pull out and a Ra < 1.6 µm. The cutting forces were low with maximal values of 15 N.

Keywords: hybrid manufacturing; green ceramics; wear monitoring; pellet additive manufacturing; milling

1. Introduction

Very hard and chemically inert materials such as ceramics find applications in a large number of industries belonging to the electrical, mechanical, chemical as well as biomedical sectors [1, 2]. Indeed, some of them, such as zirconia and its derivatives (3Y-TZP, *e.g.*), offer among the highest achievable mechanical properties for ceramics with a fracture toughness between 4 MPa $\sqrt{m}$ and 12 MPa $\sqrt{m}$, while its flexural strength can reach up to 1800 MPa [3].

Four main steps compose the conventional manufacturing route for ceramics: mixing the powder with a binder, shaping, debinding and sintering [1]. However, the shaping process for creating parts made of this material (pressing or injection moulding) is still limited to relatively simple designs [2, 4]. Moreover, the costs of the post-processing operations required to achieve a smooth surface topography (Ra < 1.6 µm, *e.g.*) can reach up to 80% of the total manufacturing cost [3]. Indeed, final machining, polishing, grinding or lapping are usually applied after the sintering process. Therefore, the part has already acquired all of its properties and requires expensive tools to be finished. Neither small series of goods nor tailored parts can be obtained by the conventional process route without requiring high costs, especially when their design is complex [3].

Unconventional processes, such as additive manufacturing (AM) enable the production of small series of goods with a complex design even with ceramic materials [5]. Moreover, no specific tooling (such as moulds, *e.g.*) are required to generate different parts [2, 4]. Among the existing AM processes classified by the ISO 52900 standard, material extrusion is one of the most promising [6]. Indeed, this process is able to produce ceramic (or metallic) green parts at low cost by using the feedstock (pellets) previously developed for the ceramic injection moulding industry (CIM) [2, 7]. This derivative of material extrusion is named PAM (pellet additive manufacturing). However, despite its relative freedom of design and a large choice of materials, PAM suffers from a staircase effect and generates rough surfaces (Ra between 9 µm and 40 µm) [8]. The produced parts then also need to be finished.

Machining ceramic parts at the green stage has already proven its ability to generate smooth surfaces and tight tolerances while avoiding the risk of inducing micro cracks [9, 10].

* Corresponding author

2212-8271
10.1016/j.procir.2023.09.235

Despite the lower costs, green machining is unable to treat complex part designs [10]. Combining additive manufacturing and green machining into the same hybrid machine can overcome the disadvantages of both processes [10, 11].

Even if research is ongoing on hybrid machines, there is still a lack of data for the milling operations performed on ceramic green parts shaped by AM. Recently, a study proposed a systematic method to determine the finishing milling parameters in green ceramics obtained by additive manufacturing [12]. One of the three selected tools showed better performances to achieve Ra < 1.6 µm while producing a surface without material pull-out. No significant tool wear according to the ISO 8688 standard was observed during the test. However, the total in material milling time for this tool was limited to 3 minutes, while the abrasive nature of the feedstock can have a strong effect on the tool life. Moreover, another recent article [13] showed a strong influence of the position of milling inside a ceramic green part on the cutting forces. Only one part was used for these experiments.

This article aims to, firstly, evaluate the tool life of a milling tool from [12] initially dedicated to thermoplastics, while producing surfaces with Ra < 1.6 µm and without material pull-out (according to the industrial application foreseen for the developed manufacturing chain). Moreover, the second goal of this article is to confirm, over a greater number of parts (ten instead of one), the decreasing tendency of the cutting forces along the build direction of an AM part as first observed in [13].

Table 1. Main printing parameters used to manufacture the parts.

Nozzle diameter	1 mm
Layer thickness	0.35 mm
First layer thickness	0.17 mm
Extrusion temperature	165°C
Build platform temperature	35°C
Infill strategy	Concentric
Infill percentage	100%
Printing time	25 minutes/part

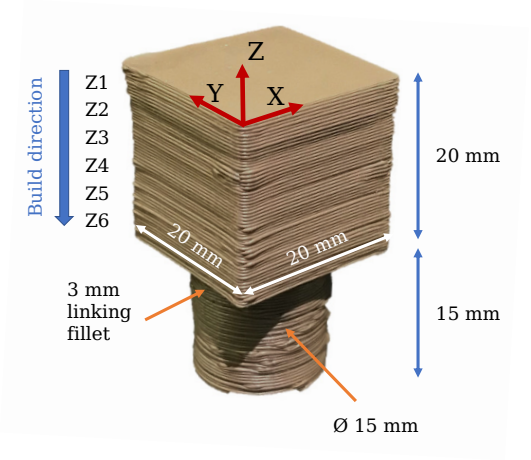

Fig. 1. As built part geometry and main dimensions.

2. Materials and method

2.1. Manufacturing of parts

The experiments were performed using ten green zirconia parts produced on a PAM printer Pollen AM Series MC in the same conditions. The feedstock used is made of 85wt% of zirconia powder (3Y-TZP) and 15wt% of thermoplastic binder (polyamide). It is commercialised with the reference K2015 by the Inmatec company (Rheinbach, Germany). The geometry of the parts and its main dimensions are given in Figure 1. It is composed of a cube on top of a cylinder, both linked by a fillet. The cube is first printed, followed by the cylinder. This allows the parts to be obtained without the need of supports structure. A reference frame is attached to the part with the Z axis along the build direction (but with the opposite orientation), and the X and Y axes following two edges of the cube. Six Z zones (from Z1 to Z6 along the Z axis) every 3 mm from the part top surface were established along the build direction as shown in Figure 1. The main printing parameters are given in Table 1.

2.2. Milling and characterisation of parts

The milling operations were performed using a robotic machining cell composed of a Stäubli TX200 robot fitted with a Teknomotor ATC71 electrospindle. The spindle can deliver up to 7.8 kW with a maximal rotational speed of 24000 rpm. The 15 mm diameter cylinder was used to clamp the part into a three-jaw chuck which was rigidly attached to a Kistler 9256C2 dynamometer.

Figure 2 shows the geometry of the selected milling tool. It is originally dedicated to the milling of thermoplastics as PA66. It is supplied by Hoffmann with the reference 209425-6 and it exhibits a 6 mm diameter, 3 teeth and a maximal cutting length of 19 mm. It is made of tungsten carbide without coating (composition was not disclosed by the tool manufacturer). As presented in a previous study [12], this tool showed great capability to generate smooth and shiny surfaces with Ra < 1.6 µm in finishing operations. The cutting conditions were selected according to the same previous study and are given in Table 2. They were obtained to complete finishing operations and to achieve the complete milling of a part in 3 min (time in material). As a result, the milling of the 10 parts took 30 minutes using the same milling tool. In total, 2400 passes were machined. No lubrication was used for the tests, while compressed air was used between the different Z zones to blow the part and evacuate the chips.

Table 2. Cutting conditions selected for the milling of parts.

Cutting speed, v_c	339 m/min
Feed rate, v_f	1458 mm/min
Axial depth of cut, a_p	3 mm
Radial depth of cut, a_e	0.5 mm
Cutting time in material	3 minutes/part

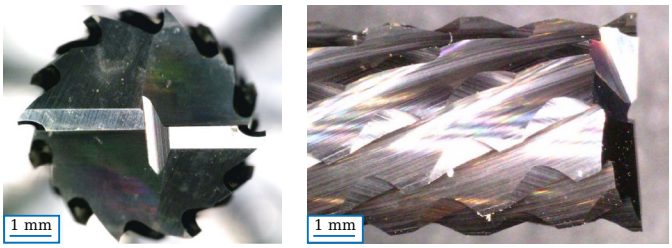

Fig. 2. Geometry of the selected milling tool, face (left) and side (right).

A Kistler 9256C2 force sensor was used to record the cutting forces for each pass at a 1800 Hz frequency. It is completed by a charge amplifier 5070A and a 5697A2 data acquisition system, both from Kistler. The reference frame of the force sensor is not the same as the one attached to the tool. Therefore, the total cutting force (Eq. 1) was considered to compare the passes of the different parts:

$$F_{tot} = \sqrt{F_X^2 + F_Y^2 + F_Z^2} \quad (1)$$

with F_X, F_Y and F_Z the force components along the X, Y and Z axes of the dynamometer, respectively.

For each part, two main steps were followed (Figure 3):

- The first step consists of carrying out eight passes (with radial and axial depths of cut according to Table 2) from the top of the cube (Z1 zone, *cf* Figure 1) following the X axis of the parts.
- The milling operation is then continued (from Z1 to Z6 zones, *cf* Figure 1) with the same radial and axial depths of cut until Step 2 is reached, with 3 mm remaining in the Y direction and 2 mm in the Z direction (Z6 zone, *cf* Figure 1). Finally, the remaining 3 mm in the Y direction are removed.

All the milling operations were carried out in conventional milling. After each step, the vertical and horizontal generated surfaces (vertical and horizontal, in brown and green respectively in Figure 3) were quantitatively and qualitatively evaluated. The cutting forces were recorded for each of the passes.

The quantitative evaluation of the surface topography was conducted with a Diavite DH6 contact rugosimeter, with parameters in accordance with the ISO 4288 standard. The arithmetic roughness was obtained with an evaluation length of 4.8 mm and a cut-off length of 0.8 mm. For all measurements, the probe was moved according to the parts X axis (feed direction of the cutting tool). The general aspect of the generated surfaces (porosities, material pull-out) was observed qualitatively using a digital microscope AM7013MZT and the DinoCapture software, both from DinoLite. Each of the horizontal and vertical surfaces were characterised by three Ra measurements at the beginning, middle and end of each pass (as shown by the black stars and yellow circles in Figure 3). In total, 120 measurements of roughness were recorded for the ten milled parts.

The tool wear was monitored using a Zeiss Axiolab5 microscope fitted with an Axiocam 208c camera (optical magnification = 10×). The flank faces of the end and side cutting edges were inspected along 0.5 mm and 3 mm, corresponding to the selected radial and axial depths of cut, respectively. Figure 4 shows the inspection zones considered in the case of the end cutting teeth. A picture was taken of the fresh tool and after each milled part. The slight binder accumulations (Figure 4) were removed by bathing the tool in an aqueous solution of acetone (98.5%) for 12h before inspecting the teeth.

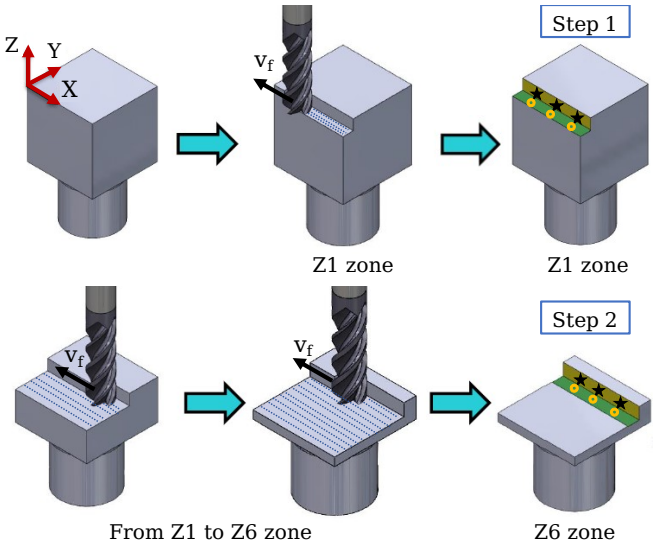

Fig. 3. Two main steps of the milling for each part.

The analysis was based on the ISO 8688 standard. Its full method cannot be applied since the material milled (green ceramic) as well as the cutting conditions (finishing) are not covered by the standard. However, it gives a clear tool life criteria for the tool with maximal values of uniform and localised flank wear of 0.3 mm and 0.5 mm, respectively. These values were used to assess the degree of wear of the selected tool.

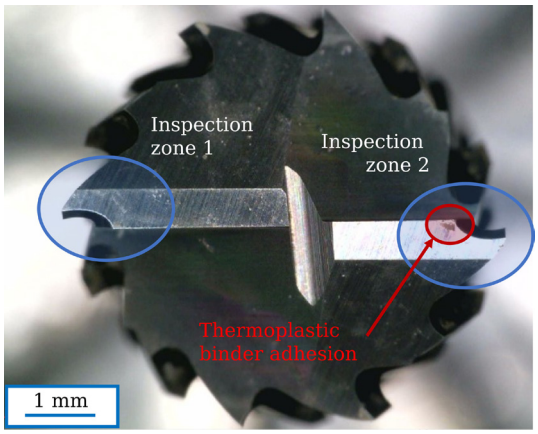

Fig. 4. Considered inspection zones for tool wear monitoring.

3. Results

3.1. Cutting forces

Figure 5 gives the evolution of the total cutting forces recorded at Z1 (the nearest to the build platform) and Z6 levels (2 mm from the cylinder in the Z direction) for each of the parts. Each bar on the graph gives the average total cutting force for 40 passes, while the $\pm\sigma$ error bars give an image of the measurement dispersion. The cutting time in material (TIM) in minutes is also given below the graph.

All the results of total cutting forces were below 15 N. From 3 min to 30 min of cutting, the average values of cutting forces slightly increased by 16% and 24% for the Z1 and Z6 zones, respectively. This can be mostly due to the appearance of wear on the tool. However, even though a slight increasing trend can be retrieved from the graph, the results between the different parts for a given Z zone are not strictly increasing. These variations can have several causes, such as the heterogeneity of mechanical properties between the different parts. Moreover, the results for the Z1 and Z6 zones exhibit up to 65% of difference for a given part. This may originate from differences of mechanical properties inside the parts (as micro-hardness, for example).

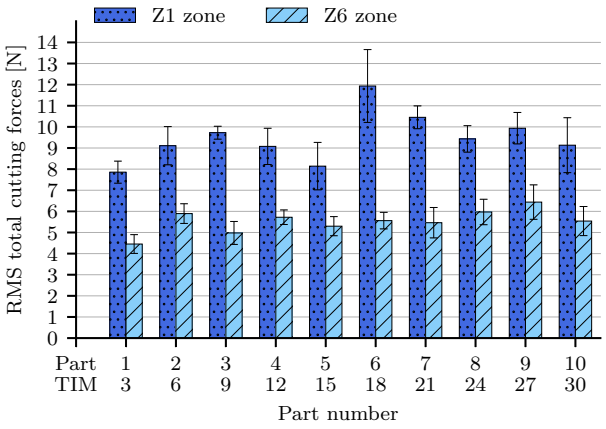

Fig. 5. Average total cutting force per part for the Z1 (the nearest from the build platform) and Z6 zones with respect to the time in material (TIM) in minutes.

Figure 6 depicts the average cutting forces from the Z1 zone to the Z6 zone for all the parts. Each bar on the graph represents 400 passes. The overall cutting forces required to machine the parts are higher in the vicinity of the build platform than further from it. Indeed, considering all the parts, the cutting forces decreased from the Z1 zone to the Z6 zone, being 58.4% lower in the Z6 zone (the furthest from the build platform) than in the Z1 zone. This confirms the tendency observed during the milling of one part by Spitaels et al. [13]. Again, the variations may originate from inhomogeneous mechanical properties (micro-hardness, *e.g.*) along the build direction. Further investigations will be required to establish their exact origin. Nevertheless, the increasing distance from the build platform from the Z1 to the Z6 zone may impact the thermal history undergone by the layers and, therefore, the binder mechanical properties. Even with these variations, the forces remained very low (below 15 N). Low cutting forces are an advantage for finishing parts directly on the build platform of the printer without using a chuck.

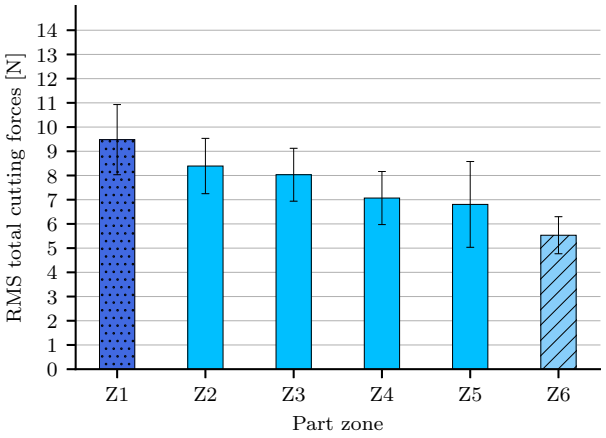

Fig. 6. Average total cutting force for all parts across the different Z zones.

3.2. Surface topography

Figure 7 gives the top and side views of the as built part as well as Parts 1 and 10, at the beginning and end of their milling respectively. The time in material (TIM) for those parts, when they are completely milled, is 3 min and 30 min.

The as built part, Figure 7 (a), shows a very rough surface topography on its sides with a Ra > 12.5 µm, while the top surface reaches values between 3.2 µm and 6.3 µm (both were estimated using a viso-tactile roughness comparator). Since the top surface is in direct contact with the build platform of the printer, it mostly acquires its surface topography.

Figure 7 (b) shows the beginning of the milling of Part 1. For the depicted pass, the milling tool only performed eight passes. As such, it is almost new. Figure 7 (c), in contrast, gives the top and side views of Part 10 at the end of its milling. The tool reached almost the 30 min of TIM. However, comparing the passes realised in Parts 1 and 10, no significant change can be observed. Indeed, the generated surface is smooth and light reflective. No material pull-out was observed in these passes as well as in the other milled parts. Therefore, the tool showed a great capability of generating the desired surface finish.

Figures 8 and 9 give the mean arithmetic roughness measured on the horizontal and vertical generated surfaces, respectively. Each graph depicts the results of the two considered zones, Z1 and Z6, with respect to the TIM and part number. The maximal allowed arithmetic roughness (Ra = 1.6 µm) is given by a red line. Each graph bar represents the average of three measurements.

As shown in Figure 8, the arithmetic roughness of the horizontal surface always belongs to the 0.8 µm Ra class (given by a blue line), except for the measurements made on Part 10. However, all the measurements were below the maximal allowed Ra

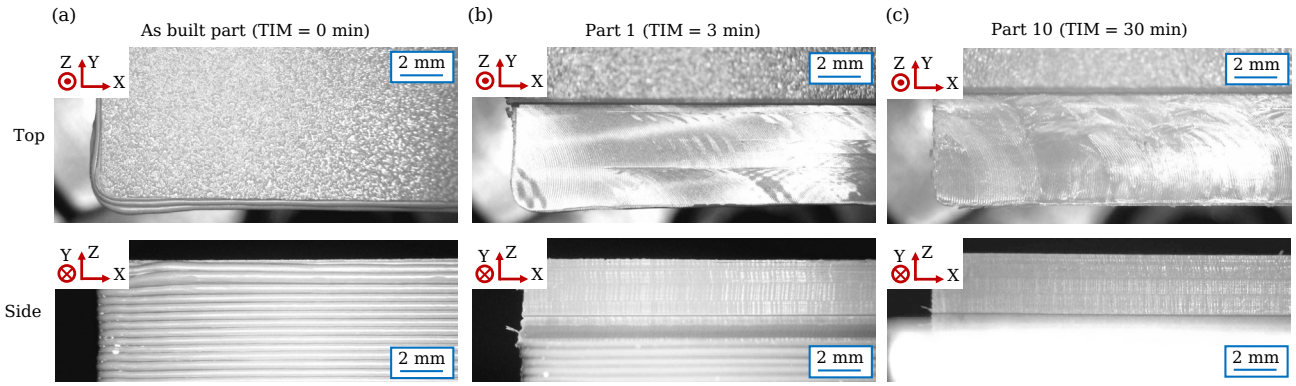

Fig. 7. Qualitative evaluation of the surface topography for the as-built part (a, TIM = 0 min), Part 1 (b, TIM = 3 min) and Part 10 (c, TIM = 30 min).

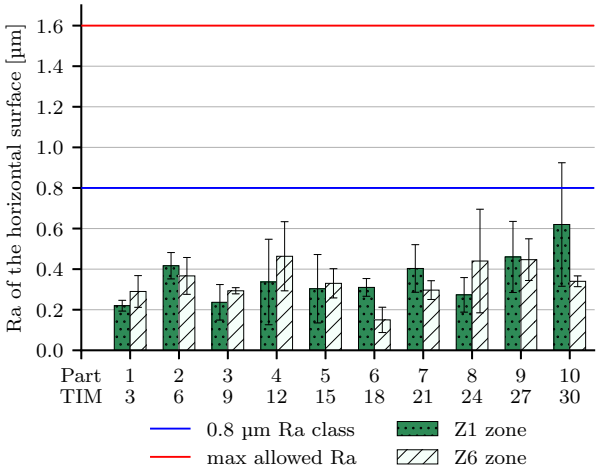

Fig. 8. Arithmetic roughness of the generated horizontal surface for the Z1 and Z6 zones depending on the part considered and the time in material (TIM).

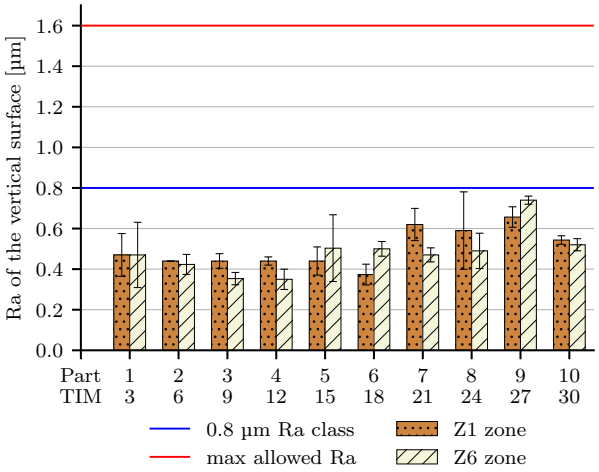

Fig. 9. Arithmetic roughness of the generated vertical surface for the Z1 and Z6 zones depending on the part considered and the time in material (TIM).

value of 1.6 µm. No significant difference (change of Ra class) can be seen between the results of the Z1 and Z6 zones, as expected according to [13]. This shows the capability of the tool to generate the desired surface topography. Even though variations can be seen in the results, the global trend is increasing. This agrees with the occurrence of progressive tool wear.

The same observation can be made for the arithmetic roughness of the generated vertical surface. Again, all the measurements were below the 1.6 µm maximum threshold. Moreover, in this case, all the results were within the 0.8 µm Ra class. However, the Ra levels achieved are higher than those for the horizontal surface. Since the tool side and end edges exhibit different geometries, they will not give the same level of Ra. Again, no significant difference (Ra class change) can be seen between the Z1 and Z6 zones. Nevertheless, the results of these two zones for each part are closer than in the case of the horizontal surface. The general trend of Ra when the TIM increases is, in the same way, increasing. This is, again, in accordance with a progressive wear of the tool.

3.3. Wear of the cutting tool

Figure 10 (a) and (b) depict the Inspection Zones 1 and 2 of the end cutting edges for the initial tool and after 30 min of milling. In both zones, after 30 min of cutting, the tool exhibits smoothed edges (in white) and a limited wear. Figure 10 (c) gives the wear evolution for both zones: only about 0.06 mm was removed from the tool in Zone 1 and 0.05 mm in Zone 2. This explains why the Ra measured after 30 min of cutting is still very good for the generated horizontal surface, while the cutting forces slightly increased for the Z1 and Z6 zones.

Even if the wear is lower than the maximal values of the ISO 8688 (0.3 mm and 0.5 mm for the uniform and localised wear), some distance should be taken from the standard tool life criteria. Indeed, with a localised wear of 0.5 mm, the end cutting edges of the selected tool geometry will completely disappear.

Additionally, no significant wear appeared on the side cutting edges. Indeed, less than 0.03 mm was removed from the tool. Again, this explain why Ra is still good (below 0.8 µm) for the generated vertical surface even after 30 minutes of milling.

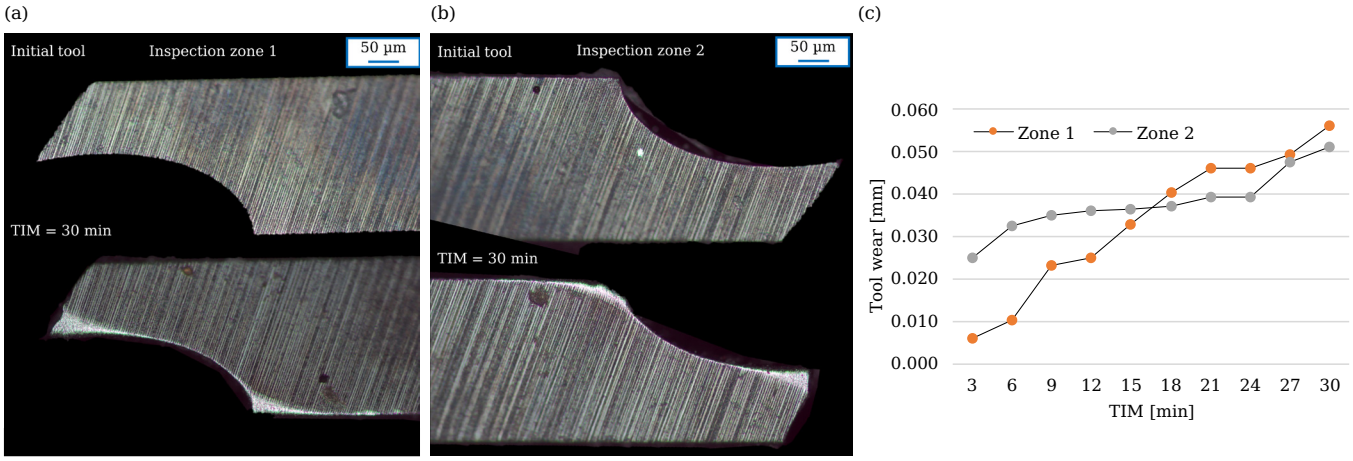

Fig. 10. Wear Inspection Zones 1 (a) and 2 (b) for the initial tool (top) and after 30 min of milling (bottom), and wear evolution for these zones (c).

The low wear observed shows that the tool can withstand the finishing operations with the selected cutting conditions without enduring catastrophic damage.

4. Conclusions

Finishing milling of zirconia green parts shaped by the PAM process was conducted with a tool initially dedicated to thermoplastic materials. The main conclusions of the study are:

- The tool can withstand 30 minutes of finishing milling using a cutting speed of 339 m/min and a feed rate of 1458 mm/min. Neither catastrophic wear nor a significant degradation of the generated surfaces was observed.
- The low cutting forces (< 15 N) enable the finishing of the parts directly in the printer to be foreseen. A decreasing trend was observed following the build direction. The differences of mechanical properties resulting from the thermal history undergone by the layers may explain this tendency. However, extra investigations are needed to establish its exact cause.
- All Ra results were below 1.6 µm. The generated vertical surfaces, compared to the horizontal, showed higher values of Ra. No material pull-out occurred, while the surfaces were smooth and light reflective.
- The measured wear was limited (below 0.1 mm, so under the ISO 8688 tool life criteria) for the end and side cutting edges, showing the ability of the tool to withstand the cutting conditions.

Acknowledgements

The Walloon regional government funded this research under the grant: 2110084 (HyProPAM research project).

References

[1] Galusek, D., Ghillányová, K., 2014. Ceramic Oxides, in "*Ceramics Science and Technology*". In: Riedel, R., Chen, I.W. (Eds.). Wiley-VCH Verlag GmbH & Co., pp. 1–58.
[2] Altiparmak, S.C., Yardley, V.A., Shi, Z., Lin, J., 2022. Extrusion-based additive manufacturing technologies: State of the art and future perspectives. J. Manuf. Process. 83, pp. 607–636.
[3] Ferraris, E., Vleugels, J., Guo, Y., Bourell, D., Kruth, J.P., Lauwers, B., 2016. Shaping of engineering ceramics by electro, chemical and physical processes. CIRP Ann.-Manuf. Technol. 65, pp. 761–784.
[4] Ferrage, L., Bertrand, G., Lenormand, P., Grossin, D., Ben-Nissan, B., 2017. A review of the additive manufacturing (3DP) of bioceramics: Alumina, zirconia (PSZ) and hydroxyapatite. J. Aust. Ceram. Soc. 53, pp. 11–20.
[5] Bourell, D., Kruth, J.P., Leu, M., Levy, G., Rosen, D., Beese, A.M., Clare, A., 2017. Materials for additive manufacturing. CIRP Ann. 66, pp. 659–681.
[6] Smartech Analysis, 2018. Ceramics Additive Manufacturing Markets 2017–2028, an Opportunity Analysis and Ten-Year Market Forecast.
[7] Rane, K., Strano, M., 2019. A comprehensive review of extrusion-based additive manufacturing processes for rapid production of metallic and ceramic parts. Adv. Manuf. 7, pp. 155–173.
[8] Turner, B.N., Gold, S.A., 2015.A review of melt extrusion additive manufacturing processes: II. Materials, dimensional accuracy, and surface roughness. Rapid Prototyp. J. 2015, 21, pp. 250–261.
[9] Demarbaix, A., Mulliez, M., Rivière-Lorphèvre, E., Spitaels, L., Duterte, C., Preux, N., Petit, F., Ducobu, F., 2021. Green Ceramic Machining: Determination of the Recommended Feed Rate for Y-TZP Milling. J. Compos. Sci. 5, 231.
[10] Parenti, P., Cataldo, S., Grigis, A., Covelli, M., Annoni,M., 2019. Implementation of hybrid additive manufacturing based on extrusion of feedstock and milling. Procedia Manuf. 2019, 34, pp. 738–746.
[11] Flynn, J.M., Shokrani, A., Newman, S.T., Dhokia, V., 2016. Hybrid additive and subtractive machine tools – Research and industrial developments. Int. J. Mach. Tools Manuf. 2016, 101, pp. 79–101.
[12] Spitaels, L., Dantinne, H., Bossu, J., Rivière-Lorphèvre, E., Ducobu, F., 2023. A Systematic Approach to Determine the Cutting Parameters of AM Green Zirconia in Finish Milling. J. Compos. Sci. 7, 112.
[13] Spitaels, L., Rivière-Lorphèvre, E., Martic, G., Juste, E., Ducobu, F., 2023. Machining of PAM green Y-TZP: Influence of build and in-plane directions on cutting forces and surface topography. Mat. Res. Proc. 28 pp. 1245–1253.